Effect of multi-sized dust distribution on local plasma sheath potentials

Meihong Sun, Lorin S. Matthews, Truell W. Hyde

Center for Astrophysics, Space Physics and Engineering Research, Baylor University, Waco, TX, 76798-7310, USA

Abstract

This work investigates the modification of a plasma sheath in a complex plasma due to the presence of dust particles with a specified size distribution. A self-consistent model for the plasma sheath is combined with a self-consistent dynamical code in order to determine the interaction of the dust particles with the local sheath potential and the subsequent effect on the dynamics of the particles. It is shown that the ion density in the region of levitated particles is decreased. The sheath potential in the region of levitated dust particles is also more negative which is qualitatively consistent with the experimental results of Arnas et al. (2000).

Key words: Dusty plasma sheath, multi-sized dust distribution, plasma crystal
PACS:

1 Introduction

Dusty plasmas are of interest in a variety of astrophysical and space physics environments. Dust of nanometer to micrometer size has also long been observed in plasmas utilized in industrial applications. Dust particles in such environments will collect thermal or monoenergetic ions, thermal plasma electrons, and in some cases, energetic electrons emitting secondary electrons. The particle obtains an electric charge as a result of the collection of plasma particles. In laboratory plasmas, the secondary emission processes due to radiation absorption and to high energy particle impacts are small and the dust particle is charged negatively due to high mobility of the plasma electrons as compared to ions.

In a laboratory setting, the electrostatic force created by the DC self-bias on the lower powered electrodes balances the gravitational force, dust particles can be trapped within the sheath region. If the ratio of the inter-particle

potential energy to the average kinetic energy is sufficient, the particles can form either a "liquid" structure with short range ordering or a crystalline structure known as a "Coulomb crystal" with longer range ordering. Such structures (for the micron size particle range) can in turn lead to a modification in the local sheath potential. Although sheath modification due to the presence of dust particles has been studied previously (See, e.g. Arnas et al., 2000; Wang and Sheng, 2003), most of these studies were carried out using monodisperse spheres. This condition is obviously artificial since the majority of astrophysical and plasma-processing environments contain a much more arbitrary particle size distribution.

In the present paper, we report a numerical study of the sheath modification created in the presence of micron-sized dust particles with a size distribution. These particles are charged negatively due to the primary electron current. A self-consistent model for the plasma sheath is combined with a self-consistent dynamical code (box_tree code, Richardson, 1993) in order to determine the interaction of the dust particles with the local sheath potential and the subsequent effect on the dynamics of the particles. The dust particle surface potential and charge are calculated using the orbit motion limited (OML) theory.

The model which describes the plasma sheath and the calculations of particle charge is given in Sec. 2. In Sec. 3, the box_tree code is briefly described. The simulation results are presented in Sec. 4 followed by our discussion. In Sec. 5, we give our conclusions.

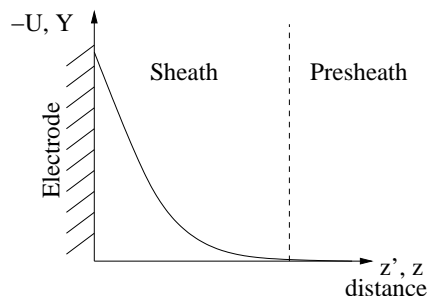## 2   Sheath model and dust particle charging

2.1   The sheath model

Fig. 1. The sheath model. The potential U is sketched as a function of z', defined as the distance from the electrode. The dimensionless variables are shown to the right of their dimensional counterparts.

The sheath region, as sketched in Fig. 1, is modeled self-consistently and considered to be collisionless. When dust particles are present, the dust space

charge effect is included in Poisson's equation

$$\nabla^2 U = -\frac{1}{\varepsilon_0}(en_i - en_e + \rho_d) \qquad (1)$$

where U is the plasma sheath potential, ε_0 is the vacuum permittivity, e is the magnitude of electronic charge, ρ_d is the dust charge density, and n_i and n_e are the ion and electron number density, respectively. Electrons react instantaneously to the sheath potential and are assumed to be in thermal equilibrium with their density given by the Boltzmann distribution

$$n_e = n_0 \exp\left(\frac{eU}{kT_e}\right). \qquad (2)$$

Ions are considered to be cold and monoenergetic with a density

$$n_i = n_0\left(1 - \frac{2eU}{m_i v_0^2}\right) \qquad (3)$$

where n_0 is the plasma density in the unperturbed plasma, m_i is the mass of the ion, and v_0 is the velocity of the ions upon entering the sheath. In this study, we assume there is an infinite supply of electrons and ions in the plasma so that the ion flux is always conserved.

Poisson's equation can be nondimensionalized by introducing the following dimensionless quantities

$$Y = -\frac{eU}{kT_e}, \; Y_d = -\frac{eU_d}{kT_e}, \; z = \frac{z'}{\lambda_D}$$

$$u_i = \frac{v_i}{c_s}, \qquad N_e = \frac{n_e}{n_0}, \qquad N_i = \frac{n_i}{n_0} \qquad (4)$$

where $\lambda_D = \sqrt{\varepsilon_0 kT_e/(e^2 n_0)}$ is the electron Debye length and $c_s = \sqrt{kT_e/m_i}$ is the ion acoustic velocity. Using Eq. (4), the governing equation Eq. (1) becomes

$$\frac{d^2Y}{dz^2} = -e^{-Y} + \left(1 + \frac{2Y}{M^2}\right)^{-1/2} + \frac{\rho_d}{en_0} \qquad (5)$$

where $M = v_0/c_s$ is the Mach number of the ion. The dimensionless boundary conditions are

$$Y(0) = Y_w, \;\; Y(\infty) = 0 \qquad (6)$$

3

where Y_w is the dimensionless wall potential. Fig. 2 shows the normalized sheath potential and electrostatic field as well as the ion density and velocity within a sheath with no dust particles present. The wall is at $z = 0$ and the sheath edge is defined as located at a position where $Y = 0.001$.
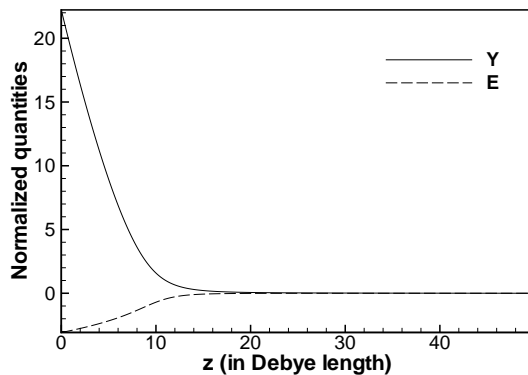
(a)
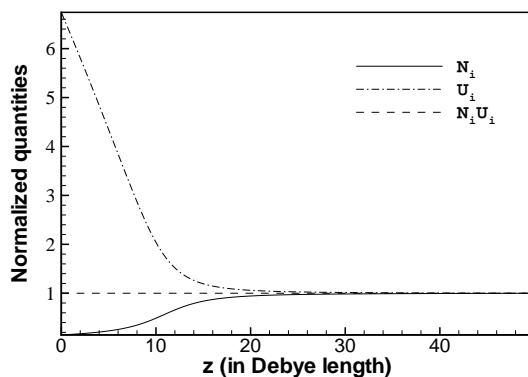
(b)

Fig. 2. (a) The normalized sheath potential and electrostatic field profiles ($Y = -eU/kT_e$, $E = dY/dz$) versus z (distance from the electrode in Debye lengths) for a collisionless sheath with no dust particles present. (b) The normalized ion density (N_i) and ion velocity (U_i). The black dashed line shows that the ion flux ($N_i U_i$) is a constant, i.e. that it is conserved.

2.2 Charging of a dust particle

The charge on a dust particle in the sheath can arise from various sources depending on the situation. However, in laboratory plasmas, the majority of these charging processes (for example, the secondary emission processes due to

radiation absorption and high energy particle impacts) are small enough that they can be neglected. As a result, we only consider charging on a dust particle to be obtained through collection of thermal plasma particles. In this case, the charge can be determined by calculating the electron and ion currents striking the particle. If the radius of the particle is smaller than the Debye length and the Debye length is less than the electron-neutral mean free path, the orbit motion limited (OML) theory (Allen, 1992) can then be used to calculate the charging currents. The equilibrium charge of a dust particle is obtained when the net current to a particle is zero

$$I_e + I_i = 0 \tag{7}$$

where I_e and I_i are the electron and ion currents respectively,

$$I_e = \begin{cases} -e\pi a^2 \left(\dfrac{8kT_e}{m_e\pi}\right)^{\frac{1}{2}} n_e \exp\left(\dfrac{eU_d}{kT_e}\right), & \text{if } \dfrac{eU_d}{kT_e} \leq 0 \\[4mm] -e\pi a^2 \left(\dfrac{8kT_e}{m_e\pi}\right)^{\frac{1}{2}} n_e \left(1 + \dfrac{eU_d}{kT_e}\right), & \text{if } \dfrac{eU_d}{kT_e} > 0 \end{cases} \tag{8}$$

$$I_i = \begin{cases} e\pi a^2 n_0 v_0 \left(1 - \dfrac{2eU_d}{m_i v_i^2}\right), & \text{if } 1 - \dfrac{2eU_d}{m_i v_i^2} \geq 0 \\[4mm] 0, & \text{if } 1 - \dfrac{2eU_d}{m_i v_i^2} < 0. \end{cases} \tag{9}$$

3 The box_tree code

The numerical code employed is based on the box_tree code developed by Richardson (1993) and later modified by Matthews and Hyde (2003, 2004) to model the dynamics of a large number of particles interacting through gravitational and electrostatic forces. The box_tree code is a hybrid of two computer algorithms, a box code and a tree code. The box code provides the external potentials acting on the grains, the linearized equations of motion, a prescription for handling boundary conditions, and specifies a coordinate system. The tree code provides a method for a fast calculation of the interparticle forces by means of a multipole expansion. The interparticle forces are then included as a perturbation to the equations of motion. Additional modifications were made to the code to allow for modeling the sheath, varying charges on the grains, and including electrostatic Debye shielding and external magnetic fields. Thus a variety of environments can be examined, including strongly coupled complex plasmas such as dust crystals and coulomb clusters (Vasut and Hyde, 2001; Qiao and Hyde, 2003).

5

4 Result and Discussion

4.1 Case 1: Monodisperse dust particles: $N = 4927, r = 4.445 \pm .04\,\mu m$

In Case 1, 4927 particles are added into the sheath. The particle sizes are $8.89 \pm .08\,\mu m$ in diameter with a density of $1.51\,\mathrm{g/cm^3}$, which corresponds to commercially available melamine-formaldehyde spheres. The particles were initially charged to a potential of -3.9 V (Konopka et al., 2000), which gives them a charge on the order of 10^{-15} C. As can be seen in Fig. 3, because the number of dust particles is not large, the sheath is only slightly affected by the presence of the particles; however even so, it can still be seen that the sheath potential with dust particles present is more negative than the sheath potential without dust particles present. This result is consistent with experimental results from Arnas et al. (2000) and numerical simulation results from Wang and Sheng (2003). The ion density change is shown in Fig. 4. As can be seen, the particles quickly obtain their equilibrium charge and equilibrium position in the sheath after only a few oscillations (Fig. 5). Ions located near the equilibrium positions of the dust particles also show a decrease in their local density.
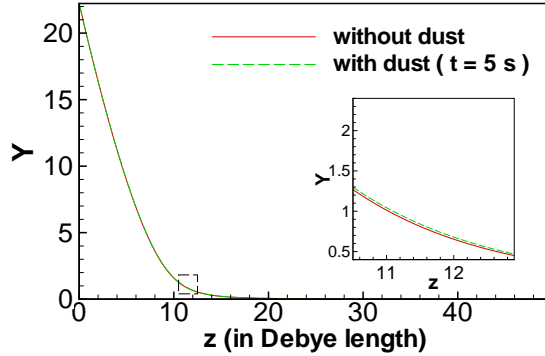

Fig. 3. Case 1: Normalized sheath potential without and with dust particles. The insert shows a enlarged view of the section marked by the box.

4.2 Case 2: Dust particles with two sizes: $N = 5206, r_1 = 4.445 \pm .04\mu m, r_2 = 3.25 \pm .04\mu m$

In case 2, equal numbers of two different sizes of dust particles are used. Because the gravitational force on smaller particles is weaker than it is on larger particles, the small particles can become trapped in a weaker electric field. As expected, it can be seen, in Fig. 6 (c), that in this case two layers of particles are formed with the smaller particles suspended above the larger. In
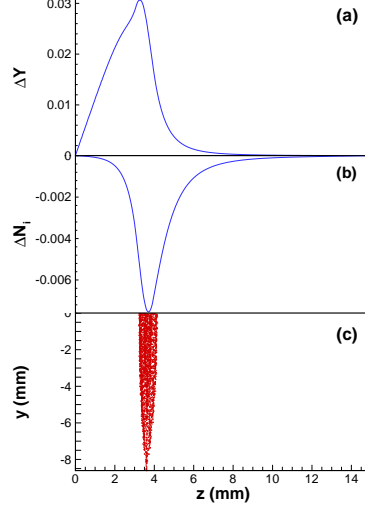
6

Fig. 4. Case 1: (a) Normalized sheath potential changes $\Delta Y = Y(t) - Y_0$, (b) ion density changes $\Delta N_i = N_i(t) - N_{i0}$ and (c) particle positions at time $t = 5\,s$ (only half of the particles are shown). (Here Y_0 and N_{i0} are the sheath potential and the ion density with no dust particles present.)
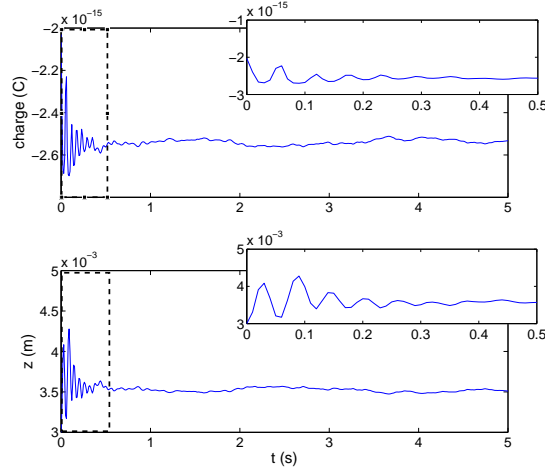

Fig. 5. Case 1: (a) Charge and (b) position for a typical dust particle (radius $r = 4.45\,\mu m$) as a function of time.

addition, the extent of the small particle distribution in the z direction is much wider than for the large particles. This is again consistent with the results of Wang and Sheng (2003) who explained this as a thermal broadening effect. The resulting changes in the sheath potential and ion density are shown in Fig. 6 (a) and (b), respectively. The particles quickly obtained their equilibrium charges and positions after several oscillations and then depleted the ions at their equilibrium positions. As seen in Fig. 7 and 8, the particles attain an equilibrium potential which is less negative than their initial potential of -3.9V.
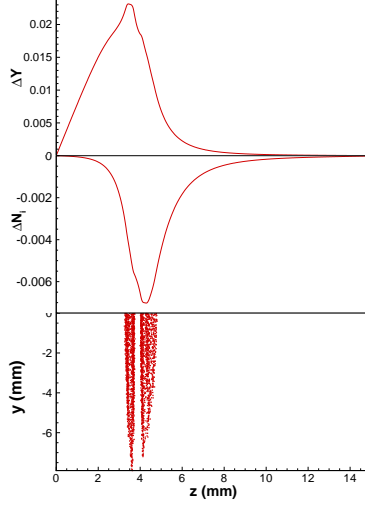
Fig. 6. Case 2: (a) Normalized sheath potential changes $\Delta Y = Y(t) - Y_0$, (b) ion density changes $\Delta N_i = N_i(t) - N_{i0}$ and (c) particle positions at time $t = 5s$ (only half of the particles are shown). The parameters are: the number of particles $N = 5206$, and the radius: $r_1 = 4.45 \pm .04\mu m$ (2603 particles) and $r_2 = 3.25 \pm .4\mu m$ (2603 particles).
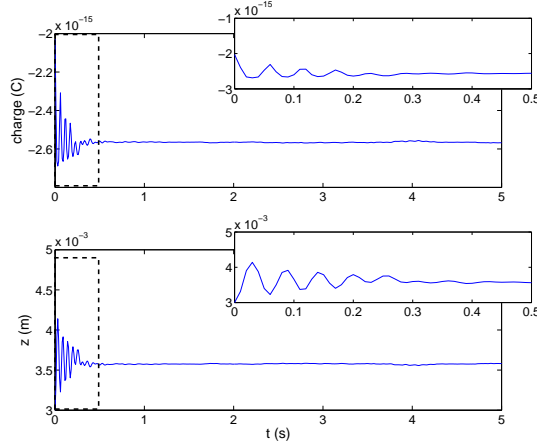

Fig. 7. Case 2: (a) Charge and (b) position for a typical large dust particle (radius $r = 4.445\mu m$) as a function of time. The inserts show enlarged views of the sections marked by the boxes.

4.3 Case 3: Dust particles with a size distribution:$N = 7926, r = 1.5 - 5.0\,\mu$
m

In Case 3, 7926 particles are added into the sheath. The particles ranged in size from $r = 1.5\,\mu$m to $r = 4.27\,\mu$m, with a size distribution peaked at $r = 2.5\,\mu$m and a particle density of 2.6 g/cm^3. These parameters correspond to commercially available glass spheres with a size distribution similar to that provided
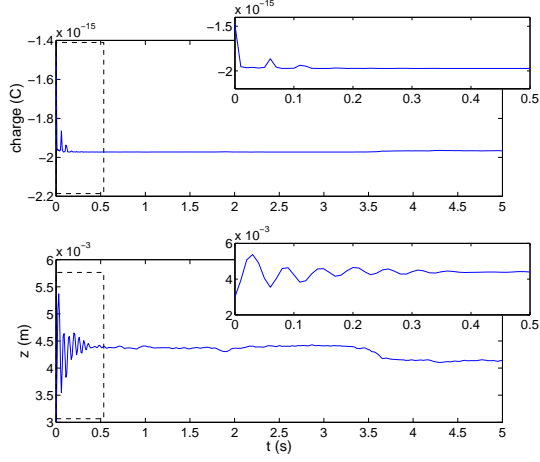
8

Fig. 8. Case 2: (a) Charge and (b) position for a typical small dust particle (radius $r = 3.251\mu m$) as a function of time. The inserts show enlarged views of the sections marked by the boxes.
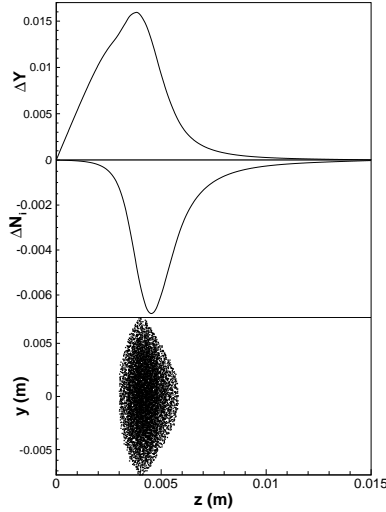

Fig. 9. Case 3: (a) Normalized sheath potential changes $\Delta Y = Y(t) - Y_0$, (b) ion density changes $\Delta N_i = N_i(t) - N_{i0}$ and (c) particle positions at time $t = 5s$.

by the manufacturer. The particles were initially charged to a potential of -3.9 V with charges ranging from -4.8×10^{-16} to -2.0×10^{-15} C. As seen in Figs. 9 and 10, the sheath modification is still not significant. The particles were again charged to a new equilibrium potential and oscillated about an equilibrium position in the sheath.
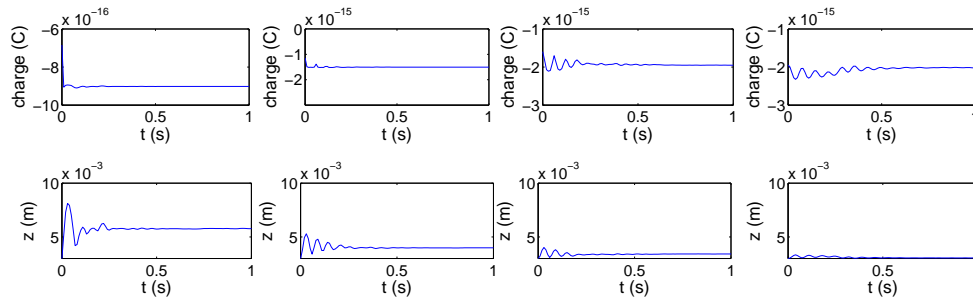
Fig. 10. Charge (a-d) and z-position (e-g) as a function of time for three typical dust particles ($r = 1.5\mu m$, $2.5\mu m$, $3.5\mu m$ $4.27\mu m$, from top to bottom) for Case 3.

5 Conclusion

We have examined the effect that three different size dust particle distributions have on a plasma sheath employing a self-consistent model and a dynamical box_tree code. The effect that a negatively charged particle size distribution has on the sheath potential was examined and it was shown that particles of different sizes levitate in the sheath at different heights with larger particles below smaller ones. The particles collect ions at their equilibrium positions with the local ion density decreased due to this effect. Since the dust particles with negative charges levitate in the sheath, the sheath potential is more negative locally in the presence of dust particles. This is consistent with the experimental results of Arnas et al. (2000) and the numerical simulation results of Wang and Sheng (2003).

References

Allen, J. E., 1992. Probe theory-the orbital motion approach. Physica Scripta 45 (5), 497–503.

Arnas, C., Mikikian, M., Bachet, G., Doveil, F., 2000. Sheath modification in the presence of dust particles. Physics of Plasmas 7 (11), 4418–4422.

Konopka, U., Morfill, G., Ratke, L., 2000. Measurement of the interaction potential of microspheres in the sheath of a rf discharge. Phys. Rev. Lett. 84 (5), 891–894.

Matthews, L., Hyde, T. W., 2003. Gravitoelectrodynamics in saturns f ring: Encounters with prometheus and pandora. J. Phys. A: Math. Gen. 36, 6207–6214.

Matthews, L., Hyde, T. W., 2004. Effects of the charge-dipole interaction on the coagulation of fractal aggregates. IEEE Transaction on Plasma Science 32 (2), 586–593.

Qiao, K., Hyde, T., 2003. Dispersion properties of the out-of-plane transverse wave in a two-dimensional coulomb crystal. Phys. Rev. E 68 (4), No. 046403.

Richardson, D., 1993. A new tree code method for simulation of planetesimal dynamics. Monthly Notices of the Royal Astronomy Society 261 (2), 396–414.

Vasut, J., Hyde, T., 2001. Computer simulations of coulomb crystallization in a dusty plasma. IEEE Transaction on Plasma Science 29 (2), 231–237.

Wang, D., Sheng, M., 2003. Effects of the trapping dust particles on the sheath structure in radio-frequency discharges. J. Appl. Phys. 94 (3), 1368–1373.